Title	Identifying a new locus that regulates the development of rete ovarian cysts in MRL/MpJ mice
Author(s)	Lee, Shin-Hyo; Ichii, Osamu; Otsuka, Saori; Hashimoto, Yoshiharu; Namiki, Yuka; Kon, Yasuhiro
Citation	Japanese Journal of Veterinary Research, 59(2&3), 79-88
Issue Date	2011-08
DOI	10.14943/jjvr.59.2-3.79
Doc URL	http://hdl.handle.net/2115/47148
Type	bulletin (article)
File Information	JJVR59-2&3_2.pdf

Instructions for use

Identifying a new locus that regulates the development of rete ovarian cysts in MRL/MpJ mice

**Shin-Hyo Lee[1), Osamu Ichii[1), Saori Otsuka[1),
Yoshiharu Hashimoto[2), Yuka Namiki[2), and Yasuhiro Kon[1,*)**

[1)Laboratory of Anatomy, Department of Biomedical Sciences, Graduate School of Veterinary Medicine, Hokkaido University, Sapporo 060–0818, Japan
[2)Office for Faculty Development and Teaching Enriched Veterinary Medicine, Graduate School of Veterinary Medicine, Hokkaido University, Sapporo 060–0818, Japan

Abstract

**MRL/MpJ (MRL) is a mouse model for autoimmune disease and develops ovarian cysts with age. The ovarian cysts originate from the rete ovarii, which is considered to be the remnant of fetal mesonephric tubules. In a previous study, we analyzed the genetic background of ovarian cysts by using backcross progenies between MRL and C57BL/6N (B6) mice. By interval mapping, suggestive linkages were detected on several chromosomes (Chrs), and a significant linkage on Chr 14 was designated as MRL Rete Ovarian Cyst (*mroc*).
In the present study, which evaluated 113 F2 intercross progenies, a significant linkage appeared on Chr 6 at the marker position *D6Mit188* (likelihood ratio statistic = 18.5). In particular, the peak regions of Chrs 6 and 14, which contain major causative loci by backcross analysis, showed close reverse interaction. From these results, a locus on Chr 6 was identified as *mroc2*, the second major locus associated with ovarian cyst formation in MRL mice.**

Key words: cystic rete ovarii, MRL/MpJ mice, *mroc2*, QTL analysis, rete ovarii

Introduction

In humans and animals, ovarian cysts are major causes of female reproductive dysfunctions. They are derived from several components of the ovary, such as ovarian surface epithelium, follicles, corpus luteum, and rete ovarii.[2,16] In veterinary medicine, ovarian disorders, including cystic changes, cause economic loss by affecting the fertility of farm animals such as cattle, sheep, and swine.[16]

The rete ovarii is homologous to the male rete testis. It is considered to be the remnant of mesonephric tubules and is composed of mesenchymal cells that have migrated from the mesonephros to the embryonic gonad.[6,24–26] While

*Corresponding author: Yasuhiro Kon, Laboratory of Anatomy, Department of Biomedical Sciences, Graduate School of Veterinary Medicine, Hokkaido University, Sapporo 060–0818, Japan
Phone and Fax: +81–11–706–5189. E-mail: y-kon@vetmed.hokudai.ac.jp

the rete system is considered to play a central role in ovary development, the rete ovarii in adults is generally a nonfunctional vestigial tissue.[4,5] However, some authors have hypothesized that the rete ovarii has a secretory role, which is supported by observations of eosinophilic and periodic acid-Schiff-positive secretion, columnar epithelium, and wide lumina of rete tubules in several species.[27] On the other hand, the rete ovarii is reportedly associated with pathological processes via lumen dilation and hyperplastic and/or hypertrophic epithelial changes in mice.[3,15,23]

MRL/MpJ (MRL) mice are the representative model for autoimmune diseases, including dermatitis, vasculitis, arthritis, and glomerulonephritis.[1,10,22] In addition to these autoimmune-mediated inflammatory characteristics, this strain shows interesting phenotypes such as active regeneration, metaphase-specific apoptosis in spermatogenesis, heat-shock resistance in spermatocytes, and the appearance of oocytes in testes.[17,20,21] Furthermore, we identified a new phenotype: spontaneous development of ovarian cysts originating from the rete ovarii in aged female MRL mice.[11] This finding suggests that MRL mice could be spontaneous models of ovarian cysts and provides fundamental information about female reproductive dysfunction.

In a previous study, to determine the susceptibility loci of MRL ovarian cysts originating from the rete ovarii, we performed quantitative trait loci (QTL) analysis using backcross progenies with C57BL/6N (B6) mice.[14] The marker positions *D3Mit182-244*, *D4Mit248*, *D6Mit316*, and *D11Mit212* show suggestive linkages to the development of ovarian cysts. The locus at the *D14Mit37* marker position on chromosome (Chr) 14, which showed significant linkage (likelihood ratio statistic [LRS] = 13.5), was designated as MRL Rete Ovarian Cyst (*mroc*). Furthermore, these findings suggest that the development of rete ovarian cysts in MRL mice is regulated by multiple loci on their autosomes.

In the present study, we analyzed F2 intercross progenies to obtain more detailed information about candidate QTLs related to the development of ovarian cysts in MRL mice. Comprehensive and accurate QTL analysis using both backcross and F2 progenies is fundamental for identifying the genes responsible for the development of rete ovarian cysts. These results would provide novel genetic information about the pathogenesis of ovarian disease in human and veterinary reproductive medicine.

Materials and Methods

Animals: Mouse MRL and B6 strains were purchased from Japan SLC Inc. (Hamamatsu, Japan), and F1 progenies from these were generated in our laboratory. A total of 113 F2 progenies were generated by an MRL × B6 cross between F1 mice of both sexes. Some F1 progenies were mated with MRL mice to produce 213 MRL × [MRL × B6] F1 backcross progenies as previously described.[14] These animals were maintained in specific pathogen-free conditions with a room temperature of 22°C ± 4°C, relative humidity of 55% ± 20%, and a 12-h light and dark cycle in the animal facility of the Graduate School of Veterinary Medicine, Hokkaido University. The mice were allowed free access to water and rodent food in pellet form. The mice were housed in an animal facility approved by the Association for Assessment and Accreditation of Laboratory Animal Care, and the project was approved by the Animal Experiment Committee of the Graduate School of Veterinary Medicine, Hokkaido University.

Phenotyping: The phenotyping of ovarian cystic change was performed according to our previous study.[14] Briefly, ovaries of F2 progenies were collected at 8 months of age, fixed with Bouin's solution overnight, processed through graded alcohol, and embedded in paraffin by a routine procedure. Serial sections 3-μm-thick by 30 μm

intervals with bilateral ovaries were cut and stained with hematoxylin and eosin by standard procedures. Only the section containing the biggest cystic rete ovarii was chosen for phenotype evaluation, photographed with a digital camera, and measured by ImageJ (NIH, http://www.nih.gov/ij/). Because we had already confirmed that the circumference of the rete ovarii reflected the severity of ovarian cysts,[14] these values were used as a quantitative trait in QTL analysis. When calculating the rete ovarii circumference in all mice, the F2 progenies with both larger values than the average B6 value and flattened epithelia were considered to show cystic changes.

Statistical analysis: The phenotype values of MRL, B6, and their progenies were evaluated by the nonparametric Kruskal-Wallis test (Schéffe's method) (Fig. 1c).

Genotyping: Genomic DNA was extracted from the spleen with a standard protocol and applied to a genome-wide scan analysis based on polymerase chain reaction (PCR), using 98 polymorphic microsatellite markers (Table 1). For 0.2- to 40.0-cM intervals (average = 15.1 cM), primer pairs of microsatellite markers were selected from the database at Mouse Genome Informatics (http://www.informatics.jax.org/).

PCR was carried out on a PCR thermal cycler (iCycler; Bio-Rad, Madison, WI, USA) with a cycling sequence of 94°C for 2 min (1 cycle) followed by 40 cycles consisting of denaturation at 94°C for 40 s, primer annealing at 58°C for 30 s, and extension at 72°C for 30 s. Taq DNA polymerase and buffers were purchased from Promega (Madison, WI, USA). The amplified samples were electrophoresed in 2% NuSieve 3:1 Agarose Gel (Cambrex Bio Science Rockland Inc., Rockland, ME, USA) or Agarose 3:1 (AMRESCO Inc., Solon, OH, USA), stained with ethidium bromide, and photographed under an ultraviolet lamp.

Genomic linkage and statistical analysis: Before

whole-genome scanning, 6 F2 mice of high trait in ascending order of rete ovarii circumference ($>$ 7,000 μm) were tested by chi-square (χ^2) analysis to identify the causative chromosomes. To identify the QTLs of ovarian cysts, the data of the trait score and genotyping were analyzed by MapManager QTXb20. The permutation tests were performed in 1-cM steps for 10,000 permutations to determine the statistically suggestive, significant, and very significant levels. Final results of interval mapping were considered to be suggestive for an LRS of 9.2, significant for an LRS of 17.2, and highly significant for an LRS of 28.8.

Among whole-genomic-locus-coded microsatellite markers, the interactive locus throughout the genome was analyzed by χ^2 statistics by MapManager QTXb20. The genotype and phenotype values of the interactive locus were investigated in detail and compared with those of the significant locus on Chr 6 by F2 QTL analysis.

Results

Histological features and distribution of ovarian cyst sizes in B6 and MRL progenies

Fig. 1 shows the histology and appearance of dilated rete ovarii in MRL, B6, F1, and F2 progenies. From 113 F2 progenies, 31 mice showed cystic changes in the rete ovarii according to our histological criteria. However, the circumference of rete ovarii varied among these mice (Fig. 1a and b). The circumferences of rete ovarii in MRL and B6 mice and their progenies were compared as shown in Fig. 1c. The average values of F2 progenies tended to be smaller than those of backcross progenies and larger than those of F1 progenies (Fig. 1c). In Fig. 1d, the individual traits of F2 progenies (n = 113) were arranged by the circumference of rete ovarii and compared with those of backcross progenies (n = 213). The trait distribution curve of F2 progenies was sharper than that of backcross progenies, and the maximum circumferences of

Table 1. List of the microsatellite markers used in the genotyping of F2 progenies. For positions of the microsatellite markers, refer to Mouse Genome Informatics.

Marker	cM	Marker	cM	Marker	cM
D1Mit64	3.67	D6Mit323	37.75	D13Mit17	7.73
D1Mit123	17.67	D6Mit105	49.71	D13Mit13	30.06
D1Mit303	31.79	D6Mit10	52.75	D13Mit260	63.73
D1Mit134	41.24	D6Mit194	62.90		
D1Mit191	52.66	D6Mit374	64.60	D14Mit10	6.41
D1Mit107	70.19			D14Mit133	16.80
D1Mit403	81.03	D7Mit178	2.02	D14Mit141	24.28
		D7Mit82	32.76	D14Mit142	27.68
D2Mit369	24.51	D7Mit105	79.29	D14Mit37	33.21
D2Mit107	65.13			D14Mit193	37.26
D2Mit148	100.49	D8Mit224	19.38	D14Mit265	50.90
		D8Mit226	23.05	D14Mit266	64.86
D3Mit130	2.55	D8Mit205	28.85		
D3Mit182	21.73	D8Mit343	39.33	D15Mit111	13.02
D3Mit244	35.01	D8Mit50	43.51	D15Mit71	37.80
D3Mit103	46.83	D8Mit248	44.99	D15Mit245	48.21
D3Mit288	52.94	D8Mit242	50.07		
D3Mit320	66.75	D8Mit211	54.51	D16Mit131	3.41
D3Mit129	80.49	D8Mit200	61.37	D16Mit140	40.30
		D8Mit56	76.14	D16Mit70	48.81
D4Mit235	3.57			D16Mit106	57.68
D4Mit178	34.92	D9Mit91	20.74		
D4Mit301	42.14	D9Mit181	46.58	D17Mit198	14.59
D4Mit145	43.30	D9Mit76	50.18	D17Mit119	38.15
D4Mit12	57.76	D9Mit18	71.49	D17Mit221	58.77
D4Mit251	69.05				
D4Mit127	80.52	D10Mit166	2.06	D18Mit177	21.39
D4Mit42	82.64	D10Mit42	39.72	D18Mit51	34.41
		D10Mit271	72.31	D18Mit186	45.63
D5Mit352	18.40				
D5Mit201	39.55	D11Mit62	5.78	D19Mit68	3.38
D5Mit101	80.16	D11Mit230	16.15	D19Mit80	18.24
		D11Mit212	54.34	D19Mit91	40.53
D6Mit166	1.99	D11Mit199	65.48	D19Mit33	51.76
D6Mit74	23.70	D11Mit48	82.96		
D6Mit33	24.42			DXMit166	28.26
D6Mit316	27.41	D12Mit185	9.85	DXMit130	55.45
D6Mit243	32.27	D12Mit136	13.00	DXMit186	76.75
D6Mit188	32.53	D12Mit158	38.14		

the rete ovarii of F2 progenies were lower than those of backcross progenies.

Genetic analysis of ovarian cysts in F2 progenies

To clarify the relationships between genotypes of F2 progenies and each chromosome locus, the χ^2 test was performed using 6 selected progenies showing large rete ovarii circumferences in ascending order. The marker position *D6Mit188*

(32.53 cM) on Chr 6 showed the most significant linkage to cystic changes in rete ovarii (Table 2).

In QTL analysis, the highest linkage above the significant level (LRS > 17.2) was detected only in Chr 6, and suggestive linkages (9.2 < LRS < 17.2) were not found in any chromosomes (Fig. 2a). Linkage details are shown in Fig. 2b. The loci at the *D6Mit188* (32.53 cM) marker position showed the highest linkage (LRS =
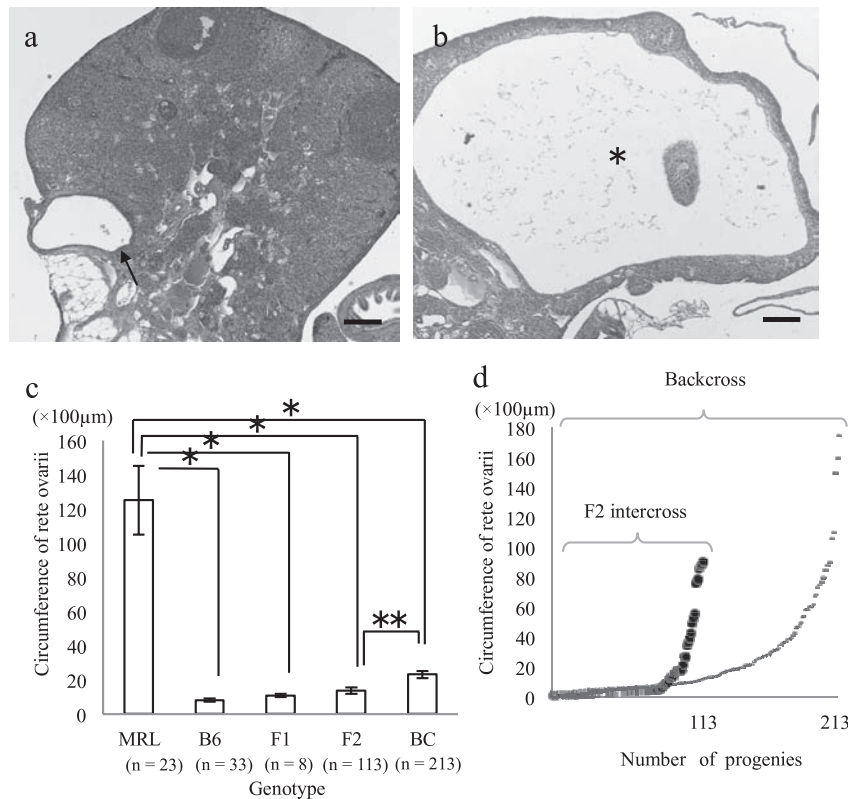
Fig. 1. Histological observation of cystic changes in murine rete ovarii of 8-month-old F2 progenies from crosses between B6 and MRL. (a) A small rete ovarian cyst (arrow) can be seen localized near the hilus. (b) Remarkable expansion of rete ovarii (asterisk) can be observed. Bars = 200 μm. (c) Average of ovarian cyst sizes in MRL, B6, (MRL × B6) F1, F2, and backcross progenies (mean ± S.E.) were evaluated by the nonparametric Kruskal-Wallis test (Schéffe's method). (*$P < 0.0001$, **$P = 0.003$). (d) Distributions of circumferences of rete ovarii in 113 F2 and 213 backcross progenies.

18.5), and *D6Mit243* (32.37 cM) and *D6Mit323* (37.75 cM) beside the peak region showed suggestive linkages to the circumference of ovarian cysts. From these results, we defined a significant locus around a suggestive locus (*D6Mit243–D6Mit323*: 32.27–37.75 cM) as a susceptibility locus of ovarian cyst development (MRL Rete Ovarian Cyst 2 [*mroc2*]).

Furthermore, the loci of *D1Mit191*, *D7Mit82*, *D12Mit185*, *D13Mit13*, *D14Mit37*, *D14Mit193*, *D14Mit265*, and *D17Mit221* interacted with *D6Mit188* in *mroc2*, showing high *P* values, according to the analysis by MapManager QTXb20 (Table 3). Above all, interaction analysis using F2 generations showed that the broad region on Chr 14 (*D14Mit37*, *D14Mit193*, and *D14Mit265*: 33.21–50.90 cM) containing the major locus *mroc* was closely related with *D6Mit188* in

mroc2. Other interactive loci not showing direct effects on the phenotype of ovarian cysts were interpreted as indirect modifier factors in the environmental background in F2 progenies.

Discussion

In this study, we analyzed the genetic locus associated with the development of MRL ovarian cysts. Our previous study using backcross progenies between MRL and B6 mice revealed that the development of ovarian cysts is regulated by polygenic factors on autosomes.[14] To obtain further genetic information about this, we compared rete ovarii circumference between the progenies formed from crosses between B6 and MRL mice. The F2 progenies composed of

Table 2. Result of the χ^2 test of the 6 most susceptible F2 progenies to ovarian cysts.

Chr	Marker	cM	Genotype M/M	B/B	M/B	χ^2	p-value	Chr	Marker	cM	Genotype M/M	B/B	M/B	χ^2	p-value
	D1Mit64	3.67	1	1	4	1.375	0.503	10	D10Mit166	2.06	0	3	3	1.375	0.503
1	D1Mit134	41.24	1	2	3	0.375	0.829		D10Mit271	72.31	3	1	2	0.375	0.829
	D1Mit403	82.03	2	2	2	0.000	1.000								
								11	D11Mit62	5.78	1	2	3	0.375	0.829
	D2Mit369	24.51	4	1	1	1.375	0.503		D11Mit48	82.96	2	2	2	0.000	1.000
2	D2Mit107	65.07	1	1	4	1.375	0.503								
	D2Mit148	100.49	0	1	5	4.375	0.112	12	D12Mit185	5.52	5	0	1	4.375	0.112
									D12Mit158	38.14	2	2	2	0.000	1.000
	D3Mit130	2.55	2	1	3	0.375	0.829								
3	D3Mit288	52.94	2	1	3	0.375	0.829	13	D13Mit17	7.73	2	3	1	0.375	0.829
	D3Mit129	80.49	2	1	3	0.375	0.829		D13Mit260	63.73	1	1	4	1.375	0.503
	D4Mit235	3.57	3	0	3	1.375	0.503		D14Mit10	6.41	2	1	3	0.375	0.829
4	D4Mit301	42.14	2	0	4	2.375	0.305	14	D14Mit37	33.21	0	2	4	2.375	0.305
	D4Mit127	80.52	1	2	3	0.375	0.829		D14Mit266	64.86	0	1	5	4.375	0.112
	D5Mit352	18.40	1	2	3	0.375	0.829	15	D15Mit111	13.02	0	1	5	4.375	0.112
5	D5Mit201	39.55	1	1	4	1.375	0.502		D15Mit245	48.21	1	2	3	0.375	0.829
	D5Mit101	80.16	0	2	4	2.375	0.305								
								16	D16Mit131	3.41	1	2	3	0.375	0.829
	D6Mit166	1.99	2	1	3	0.375	0.829		D16Mit106	57.68	2	0	4	2.375	0.305
6	**D6Mit188**	**32.53**	**6**	**0**	**0**	**8.375**	**0.015**								
	D6Mit374	64.60	4	0	2	2.375	0.305	17	D17Mit198	14.59	3	1	2	0.375	0.829
									D17Mit221	58.77	0	3	3	1.375	0.503
7	D7Mit178	2.02	2	0	4	2.375	0.305								
	D7Mit105	79.29	2	3	1	0.375	0.829	18	D18Mit177	21.39	1	1	4	1.375	0.503
									D18Mit186	45.63	1	2	3	0.375	0.829
	D8Mit224	19.38	4	0	2	2.375	0.305								
8	D8Mit50	43.51	2	0	4	2.375	0.305	19	D19Mit68	3.38	1	2	3	0.375	0.829
	D8Mit56	76.14	2	0	4	2.375	0.305		D19Mit33	51.76	2	2	2	0.000	1.000
	D9Mit91	20.74	0	3	3	1.375	0.503	X	DXMit166	28.26	0	2	4	2.375	0.305
9	D9Mit18	71.49	1	3	2	0.375	0.829		DXMit186	76.75	0	1	5	4.375	0.112

Chr = Chromosome, M = MRL homozygous, B = B6 heterozygous, H/B = Heterozygous.   ※Degrees of freedom = 2

MRL/MRL or B6/B6 homozygotes or MRL/B6 heterozygotes showed smaller average and maximum rete ovarii circumferences than those of backcross progenies composed of MRL/MRL homozygotes or MRL/B6 heterozygotes. Furthermore, F1 progenies composed of MRL/B6 heterozygotes showed smaller and larger rete ovarii than F2 and backcross progenies and B6 progenies, respectively. From these findings, we considered that the dilations of rete ovarii are promoted by both MRL-derived recessive and dominant factors. In addition to the MRL genetic background, we could not eliminate the possibility that B6-derived genetic factors inhibited the rete ovary dilations.

To identify the genetic loci affecting the dilations of rete ovarii, we performed QTL analysis using F2 progenies and clarified that only marker positions from D6Mit243 to D6Mit323 (32.27–37.75 cM) on Chr 6 showed high linkage to this phenotype. In particular, D6Mit188 (32.53 cM) exceeded the significant level. Our previous QTL analysis using backcross progenies between B6 and MRL also showed a suggestive linkage on Chr 6 (24.42–32.53 cM), with the rete ovarii dilations.[14] From these findings, in addition to QTL-associated rete ovarii dilations on Chr 14 (mroc, 33.21–37.26 cM),
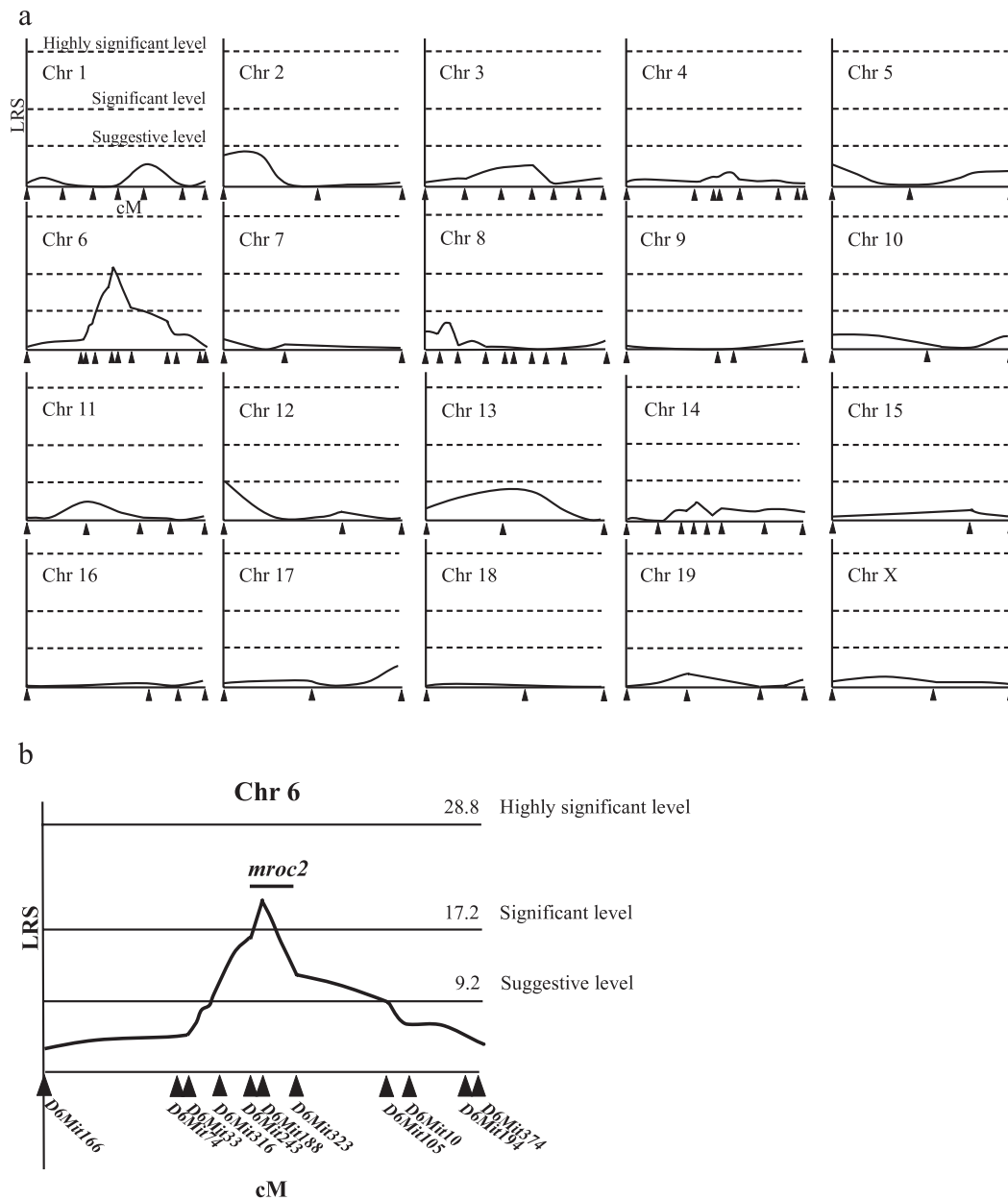
Fig. 2. Result of interval mapping in F2 progenies. (a) From the bottom, the black dotted lines represent the suggestive level (LRS score = 9.2), significant level (LRS score = 17.2), and highly significant level (LRS score = 28.8) as determined by the permutation test. Black triangles indicate the positions of microsatellite markers for each chromosome. Black solid lines indicate the LRS score (n = 113). (b) Details of significant linkages on Chr 6. *mroc2*: MRL Rete Ovarian Cyst 2.

which were found in our previous study, we named the QTL on Chr 6 (32.27–37.75 cM) in F2 analysis as *mroc2*. *mroc2* was reported to contain ovarian teratoma susceptibility loci (*Ots1*) in LT/Sv mice by (B6 × LT/Sv) F2 analysis of Chr 6 (32.53 cM).[13] Furthermore, transforming growth factor alpha, which regulates the development

and growth of the female reproductive system, is localized in the *mroc2* region (Chr 6, 37.62 cM).[7] To determine the major candidate gene affecting dilations of MRL rete ovarii, further studies focusing on qualitative and quantitative analyses of these genes on *mroc2* are required.

On the other hand, a contradiction exists,

Table 3. Interaction analysis between *mroc2* and several chromosomal positions.

mroc2 (32.27–37.75 cM)	Interaction report by MapManager QTXb20 using χ^2 test				
	Chr	cM	Locus	LRS	*p*-value	Remarks
D6Mit188 (32.53 cM)	1	52.66	*D1Mit191*	38.1	< 0.00001	
	7	32.76	*D7Mit82*	45.0		
	12	9.85	*D12Mit185*	47.7		
	13	30.06	*D13Mit13*	38.7		The *mroc* is localized at *D14Mit37* ∼ *D14Mit193*.
	14	33.21	**D14Mit37**	45.2		
	14	37.26	**D14Mit193**	40.9		
	14	50.90	*D14Mit265*	40.7		
	17	58.77	*D17Mit221*	45.6		
D6Mit243 (32.27 cM)	7	32.76	*D7Mit82*	40.6	< 0.00001	
D6Mit323 (37.75 cM)	7	32.76	*D7Mit82*	40	< 0.00001	

especially in terms of cyst severity, between F2 and backcross analyses of *mroc* and *mroc2* genotypes. Briefly, the F2 progenies having significantly larger ovarian cysts simultaneously showed MRL/MRL homozygosity on *mroc2* and B6/B6 homozygosity or MRL/B6 heterozygosity on *mroc* (Table 2). However, the backcross progenies having significantly larger rete ovarii showed MRL/B6 heterozygosity on *mroc2* and MRL/MRL homozygosity on *mroc*.[14] Although the present study could not clarify this genetic contradiction between F2 and backcross progenies, QTL and interaction analyses provided some interesting data. The loci on Chrs 1, 7, 12, 13, 14, and 17 showed significant interactions with Chr 6 (32.53 cM) on *mroc2*, and Chr 7 also showed significant interactions with Chr 6 (32.27 cM and 37.75 cM) on *mroc2*. Importantly, *D14Mit265* (50.90 cM), *D14Mit193* (37.26 cM), and *D14Mit37* (33.21 cM), which showed significant interactions with *D6Mit188* (Chr 6; 32.53 cM), contained *mroc*.[14] Furthermore, there was a possibility that these loci might directly or indirectly interact with each other, including *mroc2*. From these findings, we considered that *mroc2* in F2 progenies was affected by several autosomal loci, including *mroc*, and that the potency and balance of these genotypes determined

the severity of this polygenic phenotype. The complex interactions among genetic backgrounds through particular strain combinations cannot be easily explained; however, our results of both F2 and backcross progenies implicate the mechanisms of modifying interactions.[8,9,12,18,19]

In summary, we performed genome-wide screenings for spontaneous ovarian cysts in MRL mice. Our results indicate that the specific locus on Chr 6, named *mroc2*, is a crucial factor triggering ovarian cysts in MRL mice. Based on the fact that the QTL detected in backcross analysis did not reappear in F2 analysis, we conclude that ovarian cysts in MRL mice develop from a summation of complex genetic interactions.

References

1) Andrews, B. S., Eisenberg, R. A., Teofilopulos, A. N., Izui, S., Wilson, C. B., McConahey, P. J., Murphy, E. D., Roths, J. B. and Dixon, F. J. 1978. Spontaneous murine lupus-like syndromes. Clinical and immunopathological manifestations in several strains. *J. Exp. Med.*, **148**: 1198–1215.
2) Brassard, M., AinMelk, Y. and Baillargeon, J. P. 2008. Basic infertility including polycystic

ovary syndrome. *Med. Clin. North Am.*, **92**: 1163–1192.

3) Burdette, J. E., Oliver, R. M., Ulyanov, V., Kilen, S. M., Mayo, K. E. and Woodruff, T. K. 2007. Ovarian epithelial inclusion cysts in chronically superovulated CD1 and Smad2 dominant-negative mice. *Endocrinology*, **148**: 3595–3604.

4) Byskov, A. G. 1975. The role of the rete ovarii in meiosis and follicle formation in the cat, mink, and ferret. *J. Reprod. Fertil.*, **45**: 201–209.

5) Byskov, A. G., Skakkebaek, N. E., Stafanger, G. and Peters, H. 1977. Influence of ovarian surface epithelium and rete ovarii on follicle formation. *J. Anat.*, **123**: 77–86.

6) Byskov, A. G. 1978. The anatomy and ultrastructure of the rete system in the fetal mouse ovary. *Biol. Reprod.*, **19**: 720–735.

7) Dietrich, W. F., Miller, J., Steen, R., Merchant, M. A., Damron-Boles, D., Husain, Z., Dredge, R., Daly, M. J., Ingalls, K. A. and O'Connor, T. J. 1996. A comprehensive genetic map of the mouse genome. *Nature*, **14**: 149–152.

8) Iakoubova, O. A., Dushkin, H. and Beier, D. R. 1995. Localization of a murine recessive polycystic kidney disease mutation and modifying loci that affect disease severity. *Genomics*, **26**: 107–114.

9) Iakoubova, O. A., Dushkin, H. and Beier, D. R. 1997. Genomic analysis of a quantitative trait in a mouse model of polycystic kidney disease. *Am. J. Respir. Crit. Care Med.*, **156**: S72-S77.

10) Ichii, O., Konno, A., Sasaki, N., Endoh, D., Hashimoto, Y. and Kon, Y. 2008. Autoimmune glomerulonephritis induced in congenic mouse strain carrying telomeric region of chromosome 1 derived from MRL/MpJ. *Histol. Histopathol.*, **23**: 411–422.

11) Kon, Y., Konno, A., Hashimoto, Y. and Endoh, D. 2008. Ovarian cysts in MRL/MpJ mice originate from rete ovarii. *Anat. Histol. Embryol.*, **36**: 172–178.

12) Kuida, S. and Beier, D. R. 2000. Genetic localization of interacting modifiers affecting severity in a murine model of polycystic kidney disease. *Genome Res.*, **10**: 49–54.

13) Lee, G. H., Bugni, J. M., Obata, M., Nishimori, H., Ogawa, K. and Drinkwater, N. R. 1997. Genetic dissection of susceptibility to murine ovarian teratomas that originate from parthenogenetic oocytes. *Cancer Res.*, **57**: 590–593.

14) Lee, S. H., Ichii, O., Otsuka, S., Hashimoto, Y. and Kon, Y. 2010. Quantitative trait locus analysis of ovarian cysts derived from rete ovarii in MRL/MpJ mice. *Mamm. Genome*, **21**: 162–171.

15) Long, G. G. 2002. Apparent mesonephric duct (rete anlage) origin for cysts and proliferative epithelial lesions in the mouse ovary. *Toxicol. Pathol.*, **30**: 592–598.

16) MacLachlan, N. J. 1987. Ovarian disorders in domestic animals. *Environ. Health Perspect.*, **73**: 27–33.

17) Namiki, Y., Kon, Y., Kazusa, K., Asano, A., Sasaki, N. and Agui, T. 2004. Quantitative trait loci analysis of heat resistance of spermatocytes in the MRL/MpJ mouse. *Mamm. Genome*, **16**: 96–102.

18) Nishihara, M., Terada, M., Kamogawa, J., Ohashi, Y., Mori, S., Nakatsuru, S., Nakamura, Y. and Nose, M. 1999. Genetic basis of autoimmune sialadenitis in MRL/lpr lupus-prone mice: additive and hierarchical properties of polygenic inheritance. *Arthritis Rheumatol.*, **42**: 2616–2623.

19) Nose, M., Terada, M., Nishihara, M., Kamogawa, J., Miyazaki, T., Qu, W., Mori, S. and Nakatsuru, S. 2000. Genome analysis of collagen disease in MRL/lpr mice: polygenic inheritance resulting in the complex pathological manifestations. *Int. J. Cardiol.*, **75**: S53-S61.

20) Otsuka, S., Konno, A., Hashimoto, Y., Sasaki, N., Endoh, D. and Kon, Y. 2008. Oocytes in newborn MRL mouse testes. *Biol. Reprod.*, **79**: 9–16.

21) Otsuka, S., Namiki, Y., Ichii, O., Hashimoto, Y., Sasaki, N., Endoh, D. and Kon, Y. 2010. Analysis of factors decreasing testis weight in MRL mice. *Mamm. Genome*, **21**: 153–161.

22) Singh, R. R. 2005. SLE: translating lessons from model systems to human disease. *Trends Immunol.*, **26**: 572–579.

23) Tan, O. L., Hurst, P. R. and Fleming, J. S. 2005. Location of inclusion cysts in mouse ovaries in relation to age, pregnancy, and total ovulation number: implications for ovarian cancer? *J. Pathol.*, **205**: 483–490.

24) Upadhyay, S., Luciani, J. M. and Zamboni, L. 1979. The role of the mesonephros in the development of indifferent gonads and ovaries of the mouse. *Ann. Biol. Anim. Biochem. Biophys.*, **19**: 1179–1196.

25) Vuzquez, M. D., Bouchet, P., Mallet, J. L., Foliguet, B., Gérard, H. and LeHeup, B. 1998. 3D reconstruction of the mouse's mesonephros. *Anat. Histol. Embryol.*, **27**: 283–287.

26) Wartenberg, H. 1982. Development of the

early human ovary and role of the mesonephros in the differentiation of the cortex. *Anat. Embryol.*, **165**: 253–280.

27) Wenzel, J. S. and Odend'hal, S. 1985. The mammalian rete ovarii: a literature review. *Cornell Vet.*, **75**: 411–425.